The Journal of Chemical Physics ARTICLE scitation.org/journal/jcp

Sum-over-state expressions including second-order Herzberg–Teller effects for the calculation of absorption and resonance Raman intensities

Cite as: J. Chem. Phys. 155, 084107 (2021); doi: 10.1063/5.0057731
Submitted: 24 May 2021 • Accepted: 12 August 2021 •
Published Online: 30 August 2021

Julien Guthmuller[a)]

AFFILIATIONS

Institute of Physics and Computer Science, Faculty of Applied Physics and Mathematics, Gdańsk University of Technology, Narutowicza 11/12, 80-233 Gdańsk, Poland

[a)]Author to whom correspondence should be addressed: julien.guthmuller@pg.edu.pl

ABSTRACT

The sum-over-state expressions are derived to calculate the second-order Herzberg–Teller (HT) effects in absorption and resonance Raman spectroscopies. These effects depend on the second derivatives of the transition dipole moment with respect to the vibrational coordinates. The method is applied to the molecule of 1,3-butadiene using density functional theory calculations. It is found that the second-order HT effects are significant for both absorption and resonance Raman intensities, and that the calculated spectra are in good agreement with the experimental data. The second-order HT effects originate from diagonal elements of the second derivatives matrix, whereas non-diagonal elements have a negligible impact on the intensities of 1,3-butadiene.

I. INTRODUCTION

The spectroscopies of absorption and resonance Raman (RR) scattering are popular and efficient techniques to investigate the structure, vibrations, and the early dynamics of molecular excited states. The details and applications of these methods were reviewed in several papers and textbooks (see, e.g., Refs. 1–4). From the theoretical point of view, several approaches were developed to calculate absorption and RR intensities. Some methods are based on an explicit evaluation of the sum-over-state expression for the Raman polarizability tensor,[5–11] whereas other methods rely on a time dependent approach based on the wave packet dynamics.[12–18]

In the recent years, different studies have investigated the impact of the Herzberg–Teller (HT) effects on the intensities.[11,16,17,19–23] The HT effects are not only predominant for dipole–forbidden transitions, but they can also provide a significant contribution to the absorption and RR cross sections for dipole-allowed transitions. For example, the author of this paper investigated the first-order HT effects in *trans*-porphycene,[24] which arise from the first derivatives of the transition dipole moment. The inclusion of such effects, along with the Franck–Condon (FC) contribution, is essential to accurately predict the RR intensities of *trans*-porphycene. Similarly, the large first-order HT effects were also observed for other compounds.[16,21,22,25] The HT effects are introduced in the theory by a Taylor expansion of the transition dipole moment with respect to the vibrational coordinates. Therefore, a typical issue is whether the first-order term (depending on the first derivatives of the transition dipole moment) is sufficient to describe the HT effects or if higher-order terms (depending on the second and the higher derivatives) are necessary.[26] The present study addresses this question by extending a previous formalism[11] in order to include the second-order HT effects. The theory is derived within the frame of the independent mode displaced harmonic oscillator model, which assumes similar vibrational frequencies and modes in the ground and excited states. The sum-over-state expressions of the HT contributions are provided for the cross sections of absorption and fundamental RR transitions. Finally, the approach is applied to the molecule of 1,3-butadiene in order to illustrate the method.

II. THEORY

The formalism presented in this section provides expressions for the calculation of absorption and RR cross sections. It includes the FC contribution as well as the HT contributions arising from the first and second derivatives of the transition dipole moment. First, the main definitions and approximations are summarized. Additional details concerning these definitions can be found in previous reports,[4,11] in which first-order HT contributions were considered. Then, the final expressions of the different contributions are given for both the absorption and the RR processes.

A. Main definitions and approximations

The absorption cross section (in SI units) for transitions from the initial state $|i\rangle$ to an ensemble of the final states $|f\rangle$ is given by

$$\sigma_{Abs}(\omega_L) = \frac{\pi}{3\varepsilon_0 c\hbar}\omega_L \sum_f \sum_{\rho=\{x,y,z\}} |\langle i|\mu_\rho|f\rangle|^2 \frac{\Gamma}{\pi}\frac{1}{\left(\omega_{fi}-\omega_L\right)^2+\Gamma^2}, \quad (1)$$

where ω_L is the frequency of the incident light, $\langle i|\mu_\rho|f\rangle$ is a component of the transition dipole moment, and ω_{fi} is the Bohr frequency between the initial (i) and final (f) states. A homogeneous broadening is described by a Lorentzian function with a damping factor Γ.

The Raman differential cross section (for the commonly employed 90° scattering geometry) for a transition between the initial $|i\rangle$ and final $|f\rangle$ vibronic states is given by[1,2]

$$\frac{d\sigma_{i\to f}}{d\Omega} = \frac{\omega_L\omega_S^3}{16\pi^2\varepsilon_0^2 c^4}\frac{1}{45}(45a^2+5\delta^2+7\gamma^2), \quad (2)$$

where ω_L is the frequency of the incident light, ω_S is the frequency of the scattered light, and a^2, δ^2, and γ^2 are the three Raman invariants for randomly oriented molecules, which depend on the Raman polarizability tensor $(\alpha_{\rho\sigma})_{i\to f}$,

$$(\alpha_{\rho\sigma})_{i\to f} = \frac{1}{\hbar}\sum_k \left\{\frac{\langle f|\mu_\rho|k\rangle\langle k|\mu_\sigma|i\rangle}{\omega_{ki}-\omega_L-i\Gamma} + \frac{\langle f|\mu_\sigma|k\rangle\langle k|\mu_\rho|i\rangle}{\omega_{kf}+\omega_L+i\Gamma}\right\}, \quad (3)$$

where the index k indicates a summation over all the vibronic states of the molecule.

The following approximations are introduced:[4,11]

(i) The Born–Oppenheimer and harmonic oscillator approximations are employed.
(ii) The initial state is the electronic and vibrational ground state, i.e., $|\phi_g\rangle|\theta_{g0}\rangle$.
(iii) For the absorption process, the final states are the vibronic states of an electronic excited state (e), i.e., $|\phi_e\rangle|\theta_{ev}\rangle$, where the index v indicates the associated vibrational quantum numbers. For the RR process, fundamental transitions ($g0 \to g1_n$) are considered, i.e., the final state is $|\phi_g\rangle|\theta_{g1_n}\rangle$, where the index n indicates the mode number with a vibrational quantum number equal to 1.
(iv) In Eq. (3), the first "resonant" term in the right-hand side will dominate for an excitation frequency ω_L in close resonance with a set of vibronic states $|k\rangle$ (i.e., $\omega_L \approx \omega_{ki}$), while the second "non-resonant" term is neglected.
(v) The potential energy surfaces (PESs) of the ground and excited electronic states are described within the so-called independent mode displaced harmonic oscillator (IMDHO) model. In this case, the difference between the ground and excited state PESs is only determined by the dimensionless displacements Δ_l along the normal coordinates (q_l).

The absorption and RR cross sections depend on the transition dipole moments between the vibronic states. For example, the transition dipole moment $\langle i|\mu_\rho|k\rangle$ can be written as

$$\langle i|\mu_\rho|k\rangle = \langle\theta_{g0}|\langle\phi_g|\mu_\rho|\phi_e\rangle|\theta_{ev}\rangle = \langle\theta_{g0}|(\mu_\rho)_{ge}|\theta_{ev}\rangle, \quad (4)$$

where $(\mu_\rho)_{ge}$ is a component of the electronic transition dipole moment between the electronic ground state and the electronic excited state. $(\mu_\rho)_{ge}$ depends on the nuclear coordinates and can be developed as a Taylor series,

$$(\mu_\rho)_{ge} = (\mu_\rho)_{ge}^{eq} + \sum_l \left(\frac{\partial(\mu_\rho)_{ge}}{\partial q_l}\right)_{eq} q_l + \frac{1}{2}\sum_{l,l'}\left(\frac{\partial^2(\mu_\rho)_{ge}}{\partial q_l \partial q_{l'}}\right)_{eq} q_l q_{l'} + \cdots, \quad (5)$$

where $(\mu_\rho)_{ge}^{eq}$, $\left(\partial(\mu_\rho)_{ge}/\partial q_l\right)_{eq}$, and $\left(\partial^2(\mu_\rho)_{ge}/\partial q_l \partial q_{l'}\right)_{eq}$ are, respectively, the electronic transition dipole moment, the first derivative, and the second derivative of the electronic transition dipole moment evaluated at the ground state equilibrium geometry (denoted by eq). The expansion is performed with respect to the ground state (g) dimensionless normal coordinates q_l. In the present work, Eq. (5) is truncated after the quadratic term with respect to the normal coordinates.

In the following, simplified notations are employed for the electronic transition dipole moment and its derivatives,

$$\mu_\rho \equiv (\mu_\rho)_{ge}^{eq}, \quad (6.1)$$

$$(\mu_\rho)_l' \equiv \left(\frac{\partial(\mu_\rho)_{ge}}{\partial q_l}\right)_{eq}, \quad (6.2)$$

$$(\mu_\rho)_{ll'}'' \equiv \left(\frac{\partial^2(\mu_\rho)_{ge}}{\partial q_l \partial q_{l'}}\right)_{eq}. \quad (6.3)$$

Additionally, the dimensionless displacements for the excited state (e) are denoted as $\Delta_l \equiv \Delta_{e,l}$.

The three terms on the right-hand side of Eq. (5) are reported in Eq. (1) for the absorption and in Eq. (3) for the RR. This leads in each case to six contributions, which are denoted $[\mu\mu]$, $[\mu\mu']$, $[\mu'\mu']$, $[\mu\mu'']$, $[\mu'\mu'']$, and $[\mu''\mu'']$. The terms $[\mu\mu]$, $[\mu\mu']$, and $[\mu'\mu']$ correspond to the FC, FC/HT, and HT contributions derived in Ref. 11, respectively. The terms $[\mu\mu'']$, $[\mu'\mu'']$, and $[\mu''\mu'']$ describe the contributions arising from the second derivatives of the electronic transition dipole moment.

The dependency of the six contributions with respect to the frequency of the incident light ω_L is described by the function $\Phi_e(\omega_L)$ and by the functions $A_e(\omega_L)$, $B_e(\omega_L)$, and $C_e(\omega_L)$. The functions A_e, B_e, and C_e are expressed as the linear combinations of the Φ_e function evaluated at different frequencies (see Sec. II D).

The function $\Phi_e(\omega_L)$ is defined as[7,27]

$$\Phi_e(\omega_L) \equiv \sum_v \frac{\langle \theta_{g0}|\theta_{ev}\rangle^2}{\omega_{eg} + \omega_{v0} - \omega_L - i\Gamma}, \tag{7}$$

where the summation is taken over all the vibrational states of the electronic excited state (e), $\langle \theta_{g0}|\theta_{ev}\rangle^2$ is a FC factor, and ω_{eg} and ω_{v0} are the Bohr frequencies associated with the electronic and vibrational energies, respectively.

B. Sum-over-state expressions for the absorption cross section

By making use of the previous definitions and approximations, the absorption cross section can be written as

$$\sigma_{Abs}(\omega_L) = \frac{\omega_L}{3\varepsilon_0 c\hbar} \sum_{\rho=\{x,y,z\}} \sum_{e\neq g} \Big\{ [\mu\mu]^{Abs}_{\rho,e} + [\mu\mu']^{Abs}_{\rho,e} + [\mu'\mu']^{Abs}_{\rho,e} + [\mu\mu'']^{Abs}_{\rho,e} + [\mu'\mu'']^{Abs}_{\rho,e} + [\mu''\mu'']^{Abs}_{\rho,e} \Big\}. \tag{8}$$

The expressions for the different contributions are listed below. Moreover, the terms are separated with respect to the different orders for the displacements Δ_l, which are indicated by an additional superscript. For example, the contribution $[\mu'\mu']^{Abs}_{\rho,e}$ is the sum of the terms $[\mu'\mu']^{Abs,0}_{\rho,e}$ (order 0) and $[\mu'\mu']^{Abs,2}_{\rho,e}$ (order 2).

The FC contribution is

$$[\mu\mu]^{Abs}_{\rho,e} = \mu_\rho\mu_\rho \mathrm{Im}\{\Phi_e(\omega_L)\}. \tag{9}$$

The FC/HT contribution is

$$[\mu\mu']^{Abs}_{\rho,e} = \sum_l \mu_\rho (\mu_\rho)'_l \Delta_l \mathrm{Im}\{A_{e,l}(\omega_L)\}. \tag{10}$$

The HT contribution is

$$[\mu'\mu']^{Abs}_{\rho,e} = [\mu'\mu']^{Abs,0}_{\rho,e} + [\mu'\mu']^{Abs,2}_{\rho,e} \tag{11.1}$$

with

$$[\mu'\mu']^{Abs,0}_{\rho,e} = \frac{1}{2}\sum_l (\mu_\rho)'_l (\mu_\rho)'_l \mathrm{Im}\{\Phi_e(\omega_L - \omega_l)\}, \tag{11.2}$$

$$[\mu'\mu']^{Abs,2}_{\rho,e} = \frac{1}{4}\sum_{l,l'} (\mu_\rho)'_l (\mu_\rho)'_{l'} \Delta_l\Delta_{l'} \mathrm{Im}\{A_{e,l,l'}(\omega_L)\}. \tag{11.3}$$

The first second-order HT contribution is

$$[\mu\mu'']^{Abs}_{\rho,e} = [\mu\mu'']^{Abs,0}_{\rho,e} + [\mu\mu'']^{Abs,2}_{\rho,e} \tag{12.1}$$

with

$$[\mu\mu'']^{Abs,0}_{\rho,e} = \frac{1}{2}\sum_l \mu_\rho (\mu_\rho)''_{ll} \mathrm{Im}\{\Phi_e(\omega_L)\}, \tag{12.2}$$

$$[\mu\mu'']^{Abs,2}_{\rho,e} = \frac{1}{4}\sum_{l,l'} \mu_\rho (\mu_\rho)''_{ll'} \Delta_l\Delta_{l'} \mathrm{Im}\{A_{e,l,l'}(\omega_L)\}. \tag{12.3}$$

The second second-order HT contribution is

$$[\mu'\mu'']^{Abs}_{\rho,e} = [\mu'\mu'']^{Abs,1}_{\rho,e} + [\mu'\mu'']^{Abs,3}_{\rho,e} \tag{13.1}$$

with

$$[\mu'\mu'']^{Abs,1}_{\rho,e} = \frac{1}{2}\sum_{l,l'} (\mu_\rho)'_l (\mu_\rho)''_{ll'} \Delta_{l'} \mathrm{Im}\{B_{e,l;l'}(\omega_L)\} + \frac{1}{4}\sum_{l,l'} (\mu_\rho)'_l (\mu_\rho)''_{l'l'} \Delta_l \mathrm{Im}\{A_{e,l}(\omega_L)\}, \tag{13.2}$$

$$[\mu'\mu'']^{Abs,3}_{\rho,e} = \frac{1}{8}\sum_{l,l',l''} (\mu_\rho)'_l (\mu_\rho)''_{l'l''} \Delta_l\Delta_{l'}\Delta_{l''} \mathrm{Im}\{A_{e,l,l',l''}(\omega_L)\}. \tag{13.3}$$

The third second-order HT contribution is

$$[\mu''\mu'']^{Abs}_{\rho,e} = [\mu''\mu'']^{Abs,0}_{\rho,e} + [\mu''\mu'']^{Abs,2}_{\rho,e} + [\mu''\mu'']^{Abs,4}_{\rho,e} \tag{14.1}$$

with

$$[\mu''\mu'']^{Abs,0}_{\rho,e} = \frac{1}{8}\sum_{l,l'} (\mu_\rho)''_{ll'} (\mu_\rho)''_{ll'} \mathrm{Im}\{\Phi_e(\omega_L - \omega_l - \omega_{l'})\} + \frac{1}{16}\sum_{l,l'} (\mu_\rho)''_{ll} (\mu_\rho)''_{l'l'} \mathrm{Im}\{\Phi_e(\omega_L)\}, \tag{14.2}$$

$$[\mu''\mu'']^{Abs,2}_{\rho,e} = \frac{1}{8}\sum_{l,l',l''} (\mu_\rho)''_{ll'} (\mu_\rho)''_{ll''} \Delta_{l'}\Delta_{l''} \mathrm{Im}\{B_{e,l;l',l''}(\omega_L)\} + \frac{1}{16}\sum_{l,l',l''} (\mu_\rho)''_{ll'} (\mu_\rho)''_{l'l''} \Delta_l\Delta_{l'} \mathrm{Im}\{A_{e,l,l'}(\omega_L)\}, \tag{14.3}$$

$$[\mu''\mu'']^{Abs,4}_{\rho,e} = \frac{1}{64}\sum_{l,l',l'',l'''} (\mu_\rho)''_{ll'} (\mu_\rho)''_{l''l'''} \Delta_l\Delta_{l'}\Delta_{l''}\Delta_{l'''} \times \mathrm{Im}\{A_{e,l,l',l'',l'''}(\omega_L)\}. \tag{14.4}$$

C. Sum-over-state expressions for the resonance Raman cross section

By making use of the previous definitions and approximations, the RR polarizability tensor for fundamental transitions ($g0 \to g1_n$) can be written as

$$(\alpha_{\rho\sigma})^{RR}_{g0\to g1_n} = \frac{1}{\hbar\sqrt{2}}\sum_{e\neq g} \Big\{ [\mu\mu]^{RR}_{\rho\sigma,n,e} + [\mu\mu']^{RR}_{\rho\sigma,n,e} + [\mu'\mu']^{RR}_{\rho\sigma,n,e} + [\mu\mu'']^{RR}_{\rho\sigma,n,e} + [\mu'\mu'']^{RR}_{\rho\sigma,n,e} + [\mu''\mu'']^{RR}_{\rho\sigma,n,e} \Big\}. \tag{15}$$

The expressions for the different contributions are listed below.

The FC contribution is

$$[\mu\mu]^{RR}_{\rho\sigma,n,e} = \mu_\rho\mu_\sigma\Delta_n A_{e,n}(\omega_L). \tag{16}$$

The FC/HT contribution is

$$[\mu\mu']^{RR}_{\rho\sigma,n,e} = [\mu\mu']^{RR,0}_{\rho\sigma,n,e} + [\mu\mu']^{RR,2}_{\rho\sigma,n,e} \tag{17.1}$$

with

$$[\mu\mu']^{RR,0}_{\rho\sigma,n,e} = \mu_\rho(\mu_\sigma)'_n\Phi_e(\omega_L-\omega_n) + (\mu_\rho)'_n\mu_\sigma\Phi_e(\omega_L), \tag{17.2}$$

$$[\mu\mu']^{RR,2}_{\rho\sigma,n,e} = \frac{1}{2}\sum_l\{\mu_\rho(\mu_\sigma)'_l + (\mu_\rho)'_l\mu_\sigma\}\Delta_n\Delta_l A_{e,n,l}(\omega_L). \tag{17.3}$$

The HT contribution is

$$[\mu'\mu']^{RR}_{\rho\sigma,n,e} = [\mu'\mu']^{RR,1}_{\rho\sigma,n,e} + [\mu'\mu']^{RR,3}_{\rho\sigma,n,e} \tag{18.1}$$

with

$$\begin{aligned}[\mu'\mu']^{RR,1}_{\rho\sigma,n,e} = {}& \frac{1}{2}\sum_l(\mu_\rho)'_n(\mu_\sigma)'_l\Delta_l A_{e,l}(\omega_L)\\ &+ \frac{1}{2}\sum_l(\mu_\rho)'_l(\mu_\sigma)'_n\Delta_l B_{e,n;l}(\omega_L)\\ &+ \frac{1}{2}\sum_l(\mu_\rho)'_l(\mu_\sigma)'_l\Delta_n B_{e,l;n}(\omega_L),\end{aligned} \tag{18.2}$$

$$[\mu'\mu']^{RR,3}_{\rho\sigma,n,e} = \frac{1}{4}\sum_{l,l'}(\mu_\rho)'_l(\mu_\sigma)'_{l'}\Delta_n\Delta_l\Delta_{l'}A_{e,n,l,l'}(\omega_L). \tag{18.3}$$

The first second-order HT contribution is

$$[\mu\mu'']^{RR}_{\rho\sigma,n,e} = [\mu\mu'']^{RR,1}_{\rho\sigma,n,e} + [\mu\mu'']^{RR,3}_{\rho\sigma,n,e} \tag{19.1}$$

with

$$\begin{aligned}[\mu\mu'']^{RR,1}_{\rho\sigma,n,e} = {}& \frac{1}{2}\sum_l\mu_\rho(\mu_\sigma)''_{nl}\Delta_l B_{e,n;l}(\omega_L) + \frac{1}{2}\sum_l(\mu_\rho)''_{nl}\mu_\sigma\Delta_l A_{e,l}(\omega_L)\\ &+ \frac{1}{4}\sum_l\{\mu_\rho(\mu_\sigma)''_{ll} + (\mu_\rho)''_{ll}\mu_\sigma\}\Delta_n A_{e,n}(\omega_L),\end{aligned} \tag{19.2}$$

$$[\mu\mu'']^{RR,3}_{\rho\sigma,n,e} = \frac{1}{8}\sum_{l,l'}\{\mu_\rho(\mu_\sigma)''_{ll'} + (\mu_\rho)''_{ll'}\mu_\sigma\}\Delta_n\Delta_l\Delta_{l'}A_{e,n,l,l'}(\omega_L). \tag{19.3}$$

The second second-order HT contribution is

$$[\mu'\mu'']^{RR}_{\rho\sigma,n,e} = [\mu'\mu'']^{RR,0}_{\rho\sigma,n,e} + [\mu'\mu'']^{RR,2}_{\rho\sigma,n,e} + [\mu'\mu'']^{RR,4}_{\rho\sigma,n,e} \tag{20.1}$$

with

$$\begin{aligned}[\mu'\mu'']^{RR,0}_{\rho\sigma,n,e} = {}& \frac{1}{2}\sum_l(\mu_\rho)'_l(\mu_\sigma)''_{nl}\Phi_e(\omega_L-\omega_n-\omega_l)\\ &+ \frac{1}{2}\sum_l(\mu_\rho)''_{nl}(\mu_\sigma)'_l\Phi_e(\omega_L-\omega_l)\\ &+ \frac{1}{4}\sum_l(\mu_\rho)'_n(\mu_\sigma)''_{ll}\Phi_e(\omega_L)\\ &+ \frac{1}{4}\sum_l(\mu_\rho)''_{ll}(\mu_\sigma)'_n\Phi_e(\omega_L-\omega_n),\end{aligned} \tag{20.2}$$

$$\begin{aligned}[\mu'\mu'']^{RR,2}_{\rho\sigma,n,e} = {}& \frac{1}{4}\sum_{l,l'}\{(\mu_\rho)'_l(\mu_\sigma)''_{ll'} + (\mu_\rho)''_{ll'}(\mu_\sigma)'_l\}\Delta_n\Delta_{l'}B_{e,l;n,l'}(\omega_L)\\ &+ \frac{1}{8}\sum_{l,l'}\{(\mu_\rho)'_n(\mu_\sigma)''_{ll'} + 2(\mu_\rho)''_{nl}(\mu_\sigma)'_{l'}\}\Delta_l\Delta_{l'}A_{e,l,l'}(\omega_L)\\ &+ \frac{1}{8}\sum_{l,l'}\{2(\mu_\rho)'_l(\mu_\sigma)''_{nl'} + (\mu_\rho)''_{ll'}(\mu_\sigma)'_n\}\Delta_l\Delta_{l'}B_{e,n;l,l'}(\omega_L)\\ &+ \frac{1}{8}\sum_{l,l'}\{(\mu_\rho)'_{l'}(\mu_\sigma)''_{ll} + (\mu_\rho)''_{ll}(\mu_\sigma)'_{l'}\}\Delta_n\Delta_{l'}A_{e,n,l'}(\omega_L),\end{aligned} \tag{20.3}$$

$$\begin{aligned}[\mu'\mu'']^{RR,4}_{\rho\sigma,n,e} = {}& \frac{1}{16}\sum_{l,l',l''}\{(\mu_\rho)'_l(\mu_\sigma)''_{l'l''} + (\mu_\rho)''_{ll'}(\mu_\sigma)'_{l''}\}\\ &\times\Delta_n\Delta_l\Delta_{l'}\Delta_{l''}A_{e,n,l,l',l''}(\omega_L).\end{aligned} \tag{20.4}$$

The third second-order HT contribution is

$$[\mu''\mu'']^{RR}_{\rho\sigma,n,e} = [\mu''\mu'']^{RR,1}_{\rho\sigma,n,e} + [\mu''\mu'']^{RR,3}_{\rho\sigma,n,e} + [\mu''\mu'']^{RR,5}_{\rho\sigma,n,e} \tag{21.1}$$

with

$$\begin{aligned}[\mu''\mu'']^{RR,1}_{\rho\sigma,n,e} = {}& \frac{1}{8}\sum_{l,l'}(\mu_\rho)''_{nl}(\mu_\sigma)''_{l'l'}\Delta_l A_{e,l}(\omega_L) + \frac{1}{16}\sum_{l,l'}(\mu_\rho)''_{ll}(\mu_\sigma)''_{l'l'}\Delta_n A_{e,n}(\omega_L) + \frac{1}{4}\sum_{l,l'}(\mu_\rho)''_{nl}(\mu_\sigma)''_{ll'}\Delta_{l'}B_{e,l;l'}(\omega_L) + \frac{1}{8}\sum_{l,l'}(\mu_\rho)''_{ll}(\mu_\sigma)''_{l'n}\Delta_{l'}B_{e,n;l'}(\omega_L)\\ &+ \frac{1}{4}\sum_{l,l'}(\mu_\rho)''_{ll'}(\mu_\sigma)''_{nl}\Delta_{l'}C_{e,n,l;l'}(\omega_L) + \frac{1}{8}\sum_{l,l'}(\mu_\rho)''_{ll'}(\mu_\sigma)''_{ll'}\Delta_n C_{e,l,l';n}(\omega_L),\end{aligned} \tag{21.2}$$

$$\begin{aligned}[\mu''\mu'']^{RR,3}_{\rho\sigma,n,e} = {}& \frac{1}{16}\sum_{l,l',l''}(\mu_\rho)''_{nl}(\mu_\sigma)''_{l'l''}\Delta_l\Delta_{l'}\Delta_{l''}A_{e,l,l',l''}(\omega_L) + \frac{1}{32}\sum_{l,l',l''}\{(\mu_\rho)''_{ll'}(\mu_\sigma)''_{l'l''} + (\mu_\rho)''_{l'l''}(\mu_\sigma)''_{ll'}\}\Delta_n\Delta_l\Delta_{l'}A_{e,n,l,l'}(\omega_L)\\ &+ \frac{1}{8}\sum_{l,l',l''}(\mu_\rho)''_{ll'}(\mu_\sigma)''_{ll''}\Delta_n\Delta_{l'}\Delta_{l''}B_{e,l;n,l',l''}(\omega_L) + \frac{1}{16}\sum_{l,l',l''}(\mu_\rho)''_{ll'}(\mu_\sigma)''_{nl''}\Delta_l\Delta_{l'}\Delta_{l''}B_{e,n;l,l',l''}(\omega_L),\end{aligned} \tag{21.3}$$

$$\left[\mu''\mu''\right]^{RR,5}_{\rho\sigma,n,e} = \frac{1}{64}\sum_{l,l',l'',l'''}(\mu_\rho)''_{ll'}(\mu_\sigma)''_{l''l'''} \times \Delta_n\Delta_l\Delta_{l'}\Delta_{l''}\Delta_{l'''}A_{e,n,l,l',l'',l'''}(\omega_L). \quad (21.4)$$

D. Definition of the functions A, B, and C

This section defines the functions A_e, B_e, and C_e appearing in the contributions reported in Secs. II A–II C. First, simplified notations are introduced for the function Φ_e,

$$\Phi \equiv \Phi_e(\omega_L), \quad (22.1)$$

$$\Phi_{l_1,\ldots,l_N} \equiv \Phi_e\left(\omega_L - \sum_{i=1}^{N}\omega_{l_i}\right), \quad (22.2)$$

where $l_1,\ldots,l_N$ are N mode numbers and $\Phi_{l_1,\ldots,l_N}$ is invariant for any permutation of the indices $l_1,\ldots,l_N$.

Using these notations, the A_e functions are defined as

$$A_{e,n}(\omega_L) \equiv \Phi - \Phi_n, \quad (23.1)$$

$$A_{e,n,l}(\omega_L) \equiv \Phi - \Phi_n - \Phi_l + \Phi_{n,l}, \quad (23.2)$$

$$A_{e,n,l,l'}(\omega_L) \equiv \Phi - \Phi_n - \Phi_l - \Phi_{l'} + \Phi_{n,l} + \Phi_{n,l'} + \Phi_{l,l'} - \Phi_{n,l,l'}, \quad (23.3)$$

$$A_{e,n,l,l',l''}(\omega_L) \equiv \Phi - \Phi_n - \Phi_l - \Phi_{l'} - \Phi_{l''} + \Phi_{n,l} + \Phi_{n,l'} + \Phi_{n,l''} + \Phi_{l,l'} + \Phi_{l,l''} + \Phi_{l',l''} - \Phi_{n,l,l'} - \Phi_{n,l,l''} - \Phi_{n,l',l''} - \Phi_{l,l',l''} + \Phi_{n,l,l',l''}, \quad (23.4)$$

$$A_{e,n,l,l',l'',l'''}(\omega_L) \equiv \Phi - \Phi_n - \Phi_l - \Phi_{l'} - \Phi_{l''} - \Phi_{l'''} + \Phi_{n,l} + \Phi_{n,l'} + \Phi_{n,l''} + \Phi_{n,l'''} + \Phi_{l,l'} + \Phi_{l,l''} + \Phi_{l,l'''} + \Phi_{l',l''} + \Phi_{l',l'''} + \Phi_{l'',l'''} - \Phi_{n,l,l'} - \Phi_{n,l,l''} - \Phi_{n,l,l'''} - \Phi_{n,l',l''} - \Phi_{n,l',l'''} - \Phi_{n,l'',l'''} - \Phi_{l,l',l''} - \Phi_{l,l',l'''} - \Phi_{l,l'',l'''} - \Phi_{l',l'',l'''} + \Phi_{n,l,l',l''} + \Phi_{n,l,l',l'''} + \Phi_{n,l,l'',l'''} + \Phi_{n,l',l'',l'''} + \Phi_{l,l',l'',l'''} - \Phi_{n,l,l',l'',l'''}. \quad (23.5)$$

The $A_{e,l_1,\ldots,l_N}(\omega_L)$ function is invariant for any permutation of the indices $l_1,\ldots,l_N$.

The B_e functions are defined as

$$B_{e,n;l}(\omega_L) \equiv \Phi_n - \Phi_{n,l}, \quad (24.1)$$

$$B_{e,n;l,l'}(\omega_L) \equiv \Phi_n - \Phi_{n,l} - \Phi_{n,l'} + \Phi_{n,l,l'}, \quad (24.2)$$

$$B_{e,n;l,l',l''}(\omega_L) \equiv \Phi_n - \Phi_{n,l} - \Phi_{n,l'} - \Phi_{n,l''} + \Phi_{n,l,l'} + \Phi_{n,l,l''} + \Phi_{n,l',l''} - \Phi_{n,l,l',l''}. \quad (24.3)$$

The $B_{e,n;l_1,\ldots,l_N}(\omega_L)$ function is invariant for any permutation of the indices $l_1,\ldots,l_N$.

The C_e function is defined as

$$C_{e,n,l;l'}(\omega_L) \equiv \Phi_{n,l} - \Phi_{n,l,l'}. \quad (25)$$

III. COMPUTATIONAL METHODS

Quantum chemical calculations were carried out for 1,3-butadiene with the GAUSSIAN 16 program.[28] All the calculations were performed in a vacuum by means of density functional theory (DFT) and time dependent DFT (TDDFT) using the B3LYP exchange correlation functional with the 6-311++G(2d,2p) basis set. The geometry, harmonic vibrational frequencies, and normal coordinates of the ground state S_0 were obtained by DFT. The C_{2h} symmetry of 1,3-butadiene was maintained in these calculations. The obtained frequencies were all positive, confirming that the S_0 geometry corresponds to a minimum of the potential energy surface. To correct the lack of anharmonicity and the approximate treatment of electron correlation, the harmonic frequencies were scaled by the factor 0.97. The vertical excitation energies and transition dipole moments of the S_1 state were computed by TDDFT. The convergence parameter (*Conver* = N) on the energy and wavefunction was set at $N = 9$. This tight criterion is used for the numerical calculation of the transition dipole moment derivatives, which requires well converged values of the transition dipole moments.

Equations (8) and (15) were implemented in a local program to calculate the absorption and RR cross sections. This necessitates the computation of the displacements Δ_l, derivatives of the transition dipole moments $(\mu_\rho)'_l$ and $(\mu_\rho)''_{ll'}$, and FC overlap integrals $\langle\theta_{g0}|\theta_{ev}\rangle$. Within the IMDHO model, the displacements were calculated from the excited state energy gradients evaluated at the S_0 geometry according to

$$\Delta_l = -\frac{1}{\omega_l}\left(\frac{\partial\Omega_{eg}}{\partial q_l}\right)_{eq}, \quad (26)$$

where Ω_{eg} is the vertical transition frequency. The FC overlap integrals were computed from the displacements using recursive relations.[29] A nearly complete convergence of the FC factors summation was obtained, with a value of $\sum_v\langle\theta_{g0}|\theta_{ev}\rangle^2 > 0.999$. The first derivatives $(\partial\Omega_{eg}/\partial q_l)_{eq}$ and $(\mu_\rho)'_l$ were calculated by a two-point numerical differentiation from the TDDFT transition frequencies and the transition dipole moments,

$$\left(\frac{\partial\Omega_{eg}}{\partial q_l}\right)_{eq} = \frac{\Omega_{eg}\left(q_l^{eq}+\Delta q_l\right) - \Omega_{eg}\left(q_l^{eq}-\Delta q_l\right)}{2\Delta q_l}, \quad (27.1)$$

$$(\mu_\rho)'_l = \frac{\mu_\rho\left(q_l^{eq}+\Delta q_l\right) - \mu_\rho\left(q_l^{eq}-\Delta q_l\right)}{2\Delta q_l}, \quad (27.2)$$

where Δq_l represents a finite displacement along the normal coordinate q_l, which is added or subtracted to the ground state geometry. Similarly, the second derivatives of the transition dipole moment were calculated with the finite difference expressions. The diagonal terms were computed from

$$(\mu_\rho)''_{ll} = \frac{1}{\Delta q_l\Delta q_l}\left[\mu_\rho\left(q_l^{eq}+\Delta q_l\right) - 2\mu_\rho + \mu_\rho\left(q_l^{eq}-\Delta q_l\right)\right], \quad (28)$$

whereas the non-diagonal terms (i.e., $l \neq l'$) were obtained from

$$(\mu_\rho)''_{ll'} = \frac{1}{2\Delta q_l \Delta q_{l'}}\left[\mu_\rho\left(q_l^{eq} + \Delta q_l, q_{l'}^{eq} + \Delta q_{l'}\right) - \mu_\rho\left(q_l^{eq} + \Delta q_l\right) - \mu_\rho\left(q_{l'}^{eq} + \Delta q_{l'}\right) + 2\mu_\rho - \mu_\rho\left(q_l^{eq} - \Delta q_l\right) - \mu_\rho\left(q_{l'}^{eq} - \Delta q_{l'}\right) + \mu_\rho\left(q_l^{eq} - \Delta q_l, q_{l'}^{eq} - \Delta q_{l'}\right)\right]. \quad (29)$$

It can be noted that the numerical calculation of the derivatives represents the main computational cost of the method, whereas the evaluation of the expressions for the absorption [Eq. (8)] and the RR [Eq. (15)] represents only a small fraction of the total computational cost. The accuracy of the calculated derivatives was checked by using two different finite displacements (Tables S1–S4) as well as by extrapolating the transition dipole moment between the S_0 and S_1 geometries and comparing the results with the direct TDDFT calculation at the S_1 geometry (Table S7).

A value of Γ equals to 500 cm^{-1} was employed in the simulation of the absorption and RR spectra. This value reproduces the experimental broadening of the absorption spectrum.[30] The adiabatic transition frequency ω_{eg} was set to the value of 46 200 cm^{-1}, which corresponds to the experimental 0–0 transition in the vapor phase.[30] The RR spectra were calculated for an excitation frequency ω_L of 46 200 cm^{-1} in exact resonance with the 0–0 transition. Finally, a Lorentzian function with a full width at half maximum of 5 cm^{-1} was employed to broaden the Raman intensities.

IV. APPLICATION TO 1,3-BUTADIENE

As an example, the theory described in Sec. II is applied to the molecule of 1,3-butadiene. The absorption and RR properties of 1,3-butadiene have been the subject of several experimental and theoretical studies.[23,30–39] This compound is considered here because of its small size, which allows the numerical calculation of the second derivatives of the transition dipole moment with a reasonable computational cost. Additionally, experimental data are available in the vapor phase, which facilitates the comparison between calculated and measured intensities.

A. Absorption spectra

The first singlet excited state ^1B_u was calculated with a vertical excitation energy of 5.63 eV. It can be noted that the basis set dependence is significant for this state and that a large basis set, such as 6-311++G(2d,2p), should be employed to obtain the converged TDDFT results. For example, the vertical excitation energy is calculated 0.3 eV higher with the smaller 6-311G(d,p) basis set, i.e., at 5.93 eV. The difference is mainly ascribed to the effects of diffuse functions in the basis set as described in Hsu *et al.*[34] As a result, the calculated value with the larger basis set (5.63 eV) is underestimated by about 0.3 eV in comparison to the experimental absorption maximum (5.92 eV) measured in the vapor phase.[30,40] This is the typical accuracy of TDDFT for linear polyene oligomers.[34]

Figure 1 presents the absorption spectra in the FC approximation ($[\mu\mu]$), including the first-order HT effects ($[\mu\mu] + (1)$), the first- and second-order HT effects ($[\mu\mu] + (1) + (2)$), and the experimental spectrum in the vapor phase. The experimental spectrum

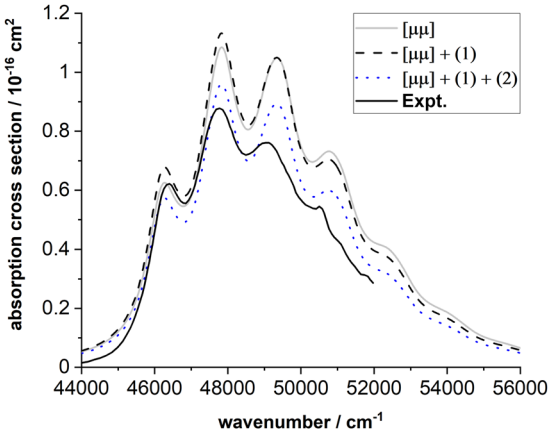

FIG. 1. Comparison between the experimental absorption spectrum[30] measured in the vapor phase (black line) and the calculated spectra in the FC approximation (gray line), including the first-order HT effects (dashed line) and the second-order HT effects (blue dotted line). (1) stands for $[\mu\mu'] + [\mu'\mu']$ and (2) stands for $[\mu\mu''] + [\mu'\mu''] + [\mu''\mu'']$.

was digitized from the spectrum reported by Phillips *et al.*[30] To correct the TDDFT inaccuracy of the excitation energy, the theoretical absorption spectra were calculated with the 0–0 transition set to the experimental value of 46 200 cm^{-1}. Moreover, the experimental broadening was simulated using a Γ equals to 500 cm^{-1}. As shown in Fig. 1, the inclusion of the first-order HT effects leads to a small increase of the cross section for the two first bands at about 46 200 and 47 800 cm^{-1}, whereas a small decrease is obtained above 50 000 cm^{-1}. The second-order HT effects have a larger impact on the spectrum than the first-order contributions, and they generate a global decrease of the absorption cross section. The vibronic structure of the experimental spectrum is properly reproduced by the calculations. Additionally, it is seen that the inclusion of the second-order HT effects improves the agreement with the experiment regarding the absolute cross section. However, the vibronic band spacing is slightly overestimated by the theory. This disagreement might originates from the neglect of frequency changes and Duschinsky mixing between the ground state and excited state vibrations,[30,31] as well as from contributions arising from the out-of-plane torsional motions.[36–39]

Figure 2 describes the effects of different terms composing the first- and second-order HT effects. The top of Fig. 2 shows that the first-order HT effects arise from the term $[\mu\mu']$, whereas the $[\mu'\mu']$ contribution has a negligible impact on the spectrum. Overall, this difference originates from the large value of the transition dipole moment in comparison to its first derivatives $(\mu_\rho)'_l$ (Tables I and S1–S4). Similarly, the bottom of Fig. 2 shows that the term $[\mu\mu'']$ dominates the second-order HT effects, whereas the $[\mu'\mu'']$ and $[\mu''\mu'']$ contributions are nearly negligible in this case.

An investigation of the contributions composing the term $[\mu\mu'']$ [Eq. (12.1)] demonstrates that the second-order HT effects arise almost entirely from the term $[\mu\mu'']^0$ of order 0 in the displacements (Fig. 3). The term $[\mu\mu'']^0$ [Eq. (12.2)] has a comparable form as the FC term $[\mu\mu]$ [Eq. (9)], in which the dependency with respect

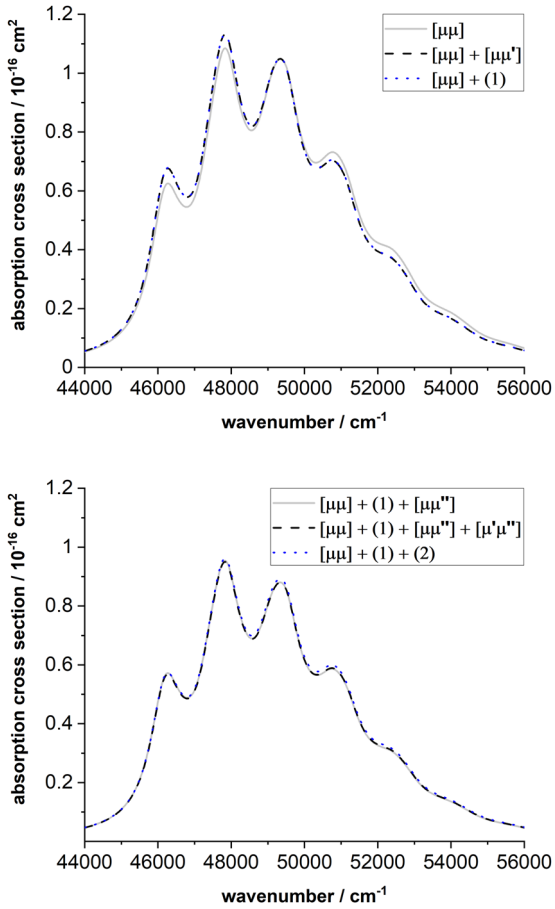

FIG. 2. Top: Comparison of absorption spectra calculated in the FC approximation (gray line), including the first-order term $[\mu\mu']$ (dashed line) and all the first-order HT effects (blue dotted line). Bottom: Comparison of spectra for the second-order HT effects, including the term $[\mu\mu'']$ (gray line), the terms $[\mu\mu'']$ + $[\mu'\mu'']$ (dashed line), and all the second-order HT effects (blue dotted line). (1) stands for $[\mu\mu']$ + $[\mu'\mu']$ and (2) stands for $[\mu\mu'']$ + $[\mu'\mu'']$ + $[\mu''\mu'']$.

TABLE I. Vibrational frequencies (cm^{-1}), displacements Δ (dimensionless), first derivatives $(\mu_\rho)'_I$, and diagonal second derivatives $(\mu_\rho)''_{II}$ of the transition dipole moment[a] (a.u.) for the A_g modes below 3000 cm^{-1}.

	Frequencies						
Mode	Cal.[b]	Expt.[c]	Δ	$(\mu_X)'_I$	$(\mu_Y)'_I$	$(\mu_X)''_{II}$	$(\mu_Y)''_{II}$
3	504	510	0.593	−0.013	−0.026	0.001	0.005
6	873	884	−0.025	0.016	0.028	0.001	0.004
12	1193	1203	−0.620	0.026	0.045	0.001	0.005
13	1280	1283	−0.825	0.004	0.019	0.002	0.004
16	1437	1440	0.360	−0.010	−0.034	0.000	0.003
18	1647	1643	−1.629	0.029	0.082	0.004	0.015

[a]The transition dipole moment has the components $\mu_X = -0.610$ a.u. and $\mu_Y = -2.064$ a.u. at the S_0 geometry.
[b]Calculated harmonic frequencies scaled by a factor of 0.97.
[c]Experimental vibrational frequencies measured in the vapor phase.[30]

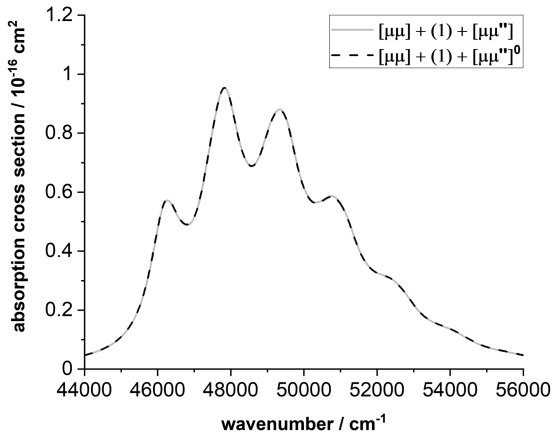

FIG. 3. Comparison of calculated absorption spectra for the second-order HT effects, including the term $[\mu\mu'']$ (gray line) and only the term $[\mu\mu'']^0$ of order 0 in the displacements (dashed line).

to the excitation frequency ω_L is given by $\mathrm{Im}\{\Phi_e(\omega_L)\}$. The dipole strength $\sum_{\rho=\{x,y,z\}}\mu_\rho\mu_\rho$ in the FC term $[\mu\mu]$ has a value of 4.632 a.u., whereas the corresponding quantity $\sum_{\rho=\{x,y,z\}}\frac{1}{2}\sum_l\mu_\rho(\mu_\rho)''_{ll}$ in the term $[\mu\mu'']^0$ is equal to −0.763 a.u. As a result, the term $[\mu\mu'']^0$ provides a negative correction to the absorption cross section. The main contribution in the summation appearing in $[\mu\mu'']^0$ [Eq. (12.2)] comes from the A_u modes (Table S2). In particular, the A_u mode calculated at 522 cm^{-1} gives a significant contribution because it has the largest diagonal second derivatives of the transition dipole moment, i.e., $(\mu_X)''_{ll}$ = 0.144 a.u. and $(\mu_Y)''_{ll}$ = 0.372 a.u. (Table S2, Fig. S1).

B. RR spectra

Table I presents the properties of the six A_g vibrational modes below 3000 cm^{-1}, while the results for the other modes are reported in Tables S1–S5. The fundamental RR transitions associated with these six A_g modes are experimentally observed for excitation wavelengths in resonance with the 0–0 absorption band.[30] The calculated vibrational frequencies are in good agreement with the experimental values, as shown by the mean absolute deviation of 6.2 cm^{-1}. The displacements and the non-zero components of the first and second derivatives of the transition dipole moment are also reported in Table I. From these values, it is expected that the RR scattering of the A_g modes is dominated by the FC contribution (i.e., term $[\mu\mu]$) because of the large value of the transition dipole moment in comparison to the values of the derivatives (Tables I and S5). Therefore, the HT effects should appear as corrections to the RR intensities obtained in the FC approximation.

Figure 4 presents RR spectra calculated for an excitation frequency in resonance with the 0–0 transition. The relative RR intensities in the FC approximation follow qualitatively the values of the squared displacements as expected from Eq. (16). The inclusion of the first-order HT effects leads to an increase of the RR intensities (Fig. 4, top), whereas the further inclusion of the second-order HT contribution produces a decrease of the RR intensities (Fig. 4,

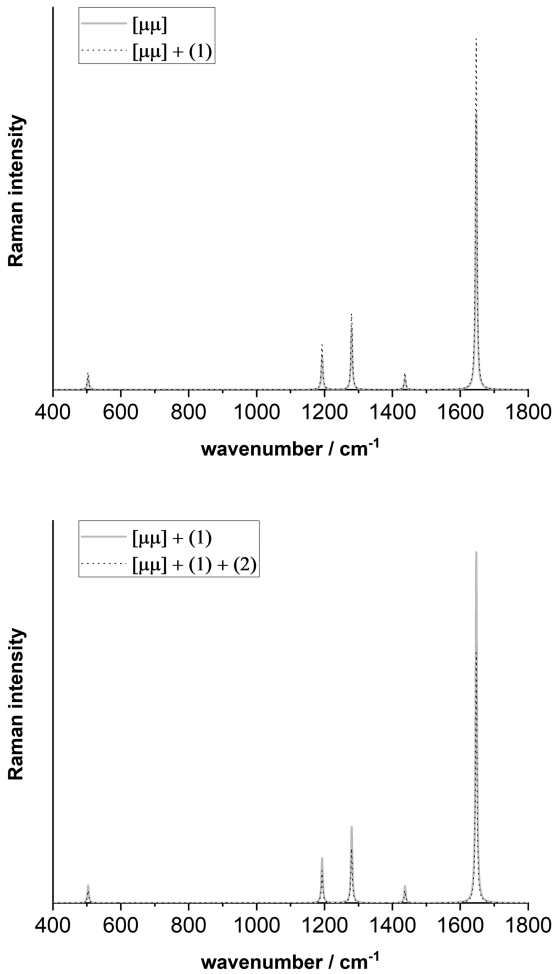

FIG. 4. Comparison of RR spectra obtained for an excitation in resonance with the 0–0 transition in the FC approximation (top: gray line), including the first-order HT effects (top: dotted line, bottom: gray line) and the second-order HT effects (bottom: dotted line). (1) stands for $[\mu\mu']+[\mu'\mu']$ and (2) stands for $[\mu\mu'']+[\mu'\mu'']+[\mu''\mu'']$.

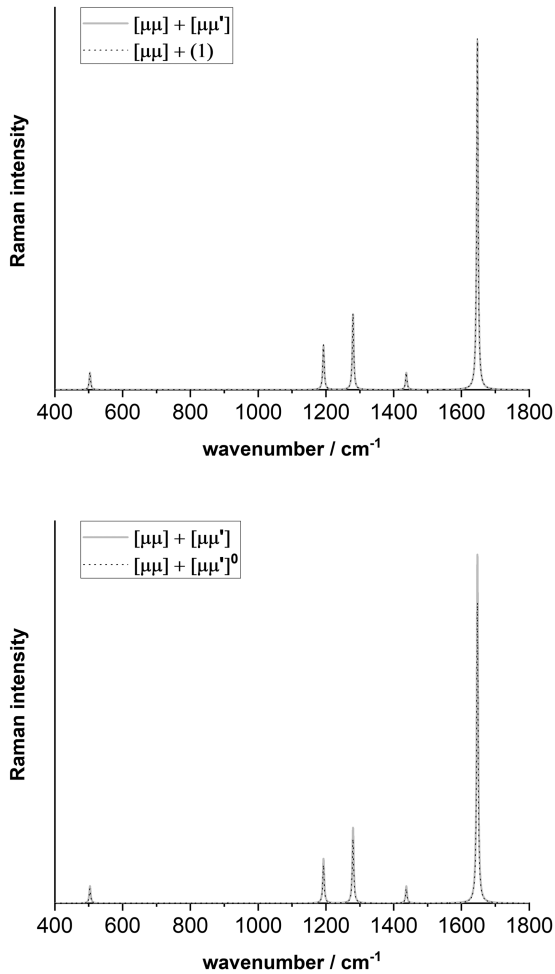

FIG. 5. Comparison of RR spectra obtained for an excitation in resonance with the 0–0 transition, including all the first-order HT effects (top: dotted line), the first-order term $[\mu\mu']$ (gray line), and only the term $[\mu\mu']^0$ of order 0 in the displacements (bottom: dotted line). (1) stands for $[\mu\mu']+[\mu'\mu']$.

bottom). This behavior correlates with the changes of intensity obtained for the first absorption band (Fig. 1). Additionally, mode 18 presents the largest variation of absolute intensity arising from the HT effects. This is due to the fact that this mode has the largest displacement as well as the largest first and second derivatives of the transition dipole moment of all A_g modes.

Figure 5 describes the impact of the different terms composing the first-order HT effects. Figure 5 (top) shows that, similar to the absorption, the first-order HT effects in the RR spectra arise from the term $[\mu\mu']$. Figure 5 (bottom) shows that both terms $[\mu\mu']^0$ and $[\mu\mu']^2$ [Eq. (17.1)] contribute to the first-order HT effects.

Figure 6 presents the effects of the different terms composing the second-order HT effects. In Fig. 6 (top-left), it is seen that the second-order HT effects originate from the term $[\mu\mu'']$. Figure 6 (top-right) reveals that only the term $[\mu\mu'']^1$ [Eq. (19.1)] of order 1 in the displacements plays a role. Moreover, Fig. 6 (bottom-left) shows the RR spectrum obtained by including only the diagonal elements of the second derivatives in the term $[\mu\mu'']^1$. It is found that the non-diagonal elements have a negligible effect. This is because only the non-diagonal elements between A_g modes contribute to the term $[\mu\mu'']^1$ [i.e., in the two first terms of Eq. (19.2), the summation runs only over the A_g modes because only these modes have non-zero displacements], and these non-diagonal elements have small values (Table S5). However, the diagonal elements of all modes contribute to the term $[\mu\mu'']^1$ via the third term of Eq. (19.2). In particular, similar to the absorption spectrum, it is found that the diagonal second derivatives of the A_u mode 4 at 522 cm^{-1} provide a significant contribution to the RR intensities of the A_g modes (Table S2 and Fig. S2). Figure 6 (bottom-right) presents a comparison between the calculated RR spectrum and the experimental spectrum in the vapor phase reconstructed from the fundamental

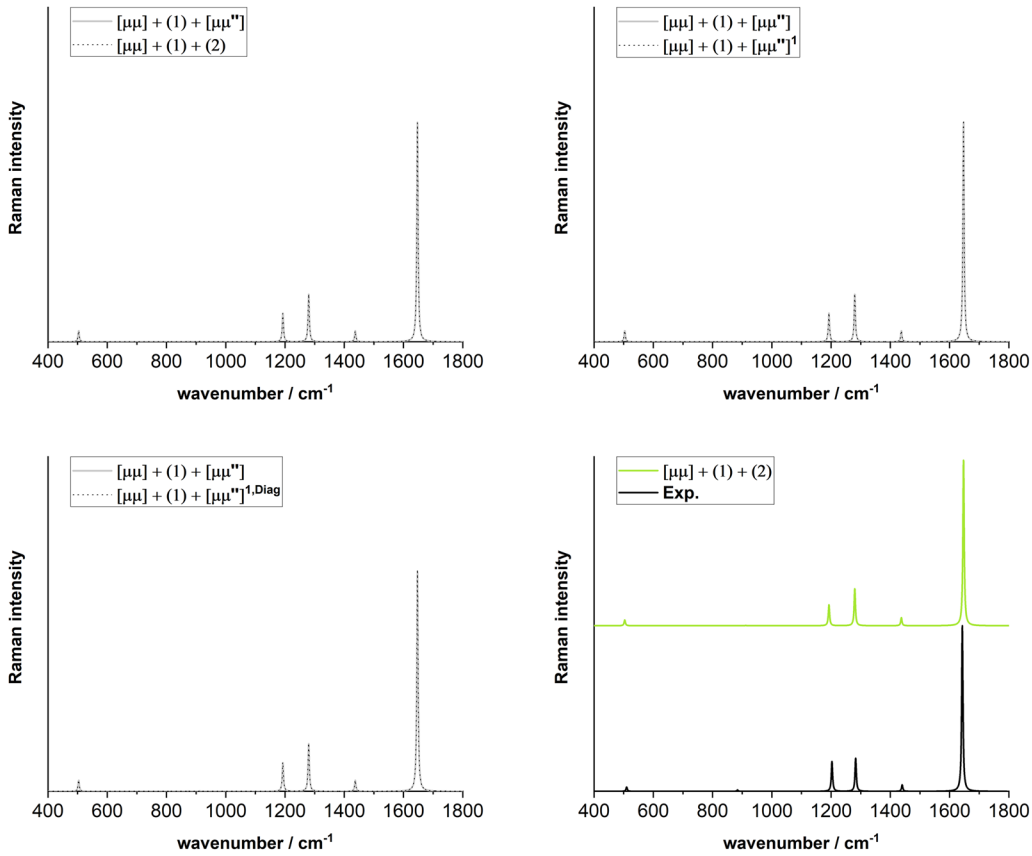

FIG. 6. Comparison of RR spectra obtained for an excitation in resonance with the 0–0 transition, including all the second-order HT effects (top-left: dotted line, bottom-right: green line), only the second-order term $[\mu\mu'']$ (gray line), only the term $[\mu\mu'']^1$ of order 1 in the displacements (top-right: dotted line), and only the term $[\mu\mu'']^1$ with diagonal second derivatives (bottom-left: dotted line). Bottom-right: Reconstructed experimental spectrum[30] in the vapor phase at an excitation wavelength of 215.0 nm (black line). (1) stands for $[\mu\mu'] + [\mu'\mu']$ and (2) stands for $[\mu\mu''] + [\mu'\mu''] + [\mu''\mu'']$.

RR intensities reported in the work of Phillips *et al.*[30] The calculated relative RR intensities are in good agreement with the experimental spectrum. The main discrepancy concerns the relative intensities of the modes 12 and 13 at 1193 and 1280 cm^{-1}, respectively. Additionally, the total RR cross section[1] calculated at 3.3×10^{-23} cm^2 for an excitation wavelength of 215.0 nm (i.e., 46 510 cm^{-1}) is in general agreement with the experimental value of 5.1×10^{-23} cm^2. It can be noted that this quantity strongly depends on the excitation frequency ω_L, for example, at an excitation frequency of 46 200 cm^{-1}, the total cross section is calculated at 4.3×10^{-23} cm^2. Furthermore, it can be mentioned that only the fundamental transitions for the A_g modes are observed in the experiment. This is in agreement with the calculations, in which the A_u, B_g, and B_u modes (Tables S2–S4) have negligible RR cross sections. In particular, the A_u mode 4 at 522 cm^{-1} can only obtain the RR intensity from terms involving non-diagonal elements of the second derivatives, which are calculated to be small. However, the overtone transition of this mode is observed in the experimental spectrum at 1044 cm^{-1} (i.e., 2×522 cm^{-1}), which indicates that the HT effects might contribute to its intensity.

V. CONCLUSIONS

In this paper, the sum-over-state expressions described in Ref. 11 have been extended in order to include the second-order HT effects. These expressions allow the calculation of the absorption spectrum as well as the RR cross section for fundamental transitions within the IMDHO model. The formulas are provided for different terms $[\mu\mu]$, $[\mu\mu']$, $[\mu'\mu']$, $[\mu\mu'']$, $[\mu'\mu'']$, and $[\mu''\mu'']$, which depend on the transition dipole moment and of its first and second derivatives with respect to the normal coordinates. Various contributions are also separated according to the different orders in the geometrical displacements Δ_l. A first application was presented for 1,3-butadiene. It was found that the calculated absorption and RR cross sections are in good agreement with the experimental spectra. Furthermore, the second-order HT effects are significant for both the absorption cross section and the absolute RR intensities. The detailed analysis of the different contributions has demonstrated that the second-order HT effects originate from the term $[\mu\mu'']^0$ in the case of absorption and from the term $[\mu\mu'']^1$ in the case of RR intensities. It was also found that the A_u modes (in particular

mode 4) mainly contribute to these terms due to their significant diagonal second derivatives. Moreover, because the HT effects are a consequence of non-adiabatic couplings, the large second-order HT effects of the A_u modes are consistent with the out-of-plane torsional motions obtained in the excited state non-adiabatic dynamics of 1,3-butadiene.[38,39] However, the non-diagonal second derivatives have a negligible effect in the case of 1,3-butadiene. If a finite difference expression is employed to calculate the first derivatives numerically [Eq. (27.2)], then the diagonal second derivatives can be obtained with nearly no additional computational cost [Eq. (28)]. Therefore, the inclusion of the second-order HT effects originating only from the diagonal second derivatives can be used as a first approximation to estimate the convergence and importance of the HT effects. This aspect can be of interest for investigating the HT effects in larger molecules, for which the calculation of the complete matrix of second derivatives might be too cumbersome.

SUPPLEMENTARY MATERIAL

See the supplementary material for additional details about the vibrational modes properties, derivatives of the transition dipole moment, absorption spectrum, and RR spectrum.

ACKNOWLEDGMENTS

The calculations have been performed at the Wrocław Centre for Networking and Supercomputing (Grant No. 384).

DATA AVAILABILITY

The data that support the findings of this study are available within the article and the supplementary material.

REFERENCES

[1] D. A. Long, *The Raman Effect: A Unified Treatment of the Theory of Raman Scattering by Molecules* (John Wiley & Sons Ltd., Chichester, 2002).
[2] A. C. Albrecht, J. Chem. Phys. **34**, 1476 (1961).
[3] M. Wächtler, J. Guthmuller, L. González, and B. Dietzek, Coord. Chem. Rev. **256**, 1479 (2012).
[4] J. Guthmuller, in *Molecular Spectroscopy: A Quantum Chemistry Approach*, edited by Y. Ozaki, M. J. Wójcik, and J. Popp (Wiley-VCH, 2019), pp. 497–536.
[5] A. Warshel and P. Dauber, J. Chem. Phys. **66**, 5477 (1977).
[6] J. Neugebauer and B. A. Hess, J. Chem. Phys. **120**, 11564 (2004).
[7] J. Guthmuller and B. Champagne, J. Chem. Phys. **127**, 164507 (2007).
[8] K. A. Kane and L. Jensen, J. Phys. Chem. C **114**, 5540 (2010).
[9] F. Santoro, C. Cappelli, and V. Barone, J. Chem. Theory Comput. **7**, 1824 (2011).
[10] S. Kupfer, M. Wächtler, J. Guthmuller, J. Popp, B. Dietzek, and L. González, J. Phys. Chem. C **116**, 19968 (2012).
[11] J. Guthmuller, J. Chem. Phys. **144**, 064106 (2016).
[12] S.-Y. Lee and E. J. Heller, J. Chem. Phys. **71**, 4777 (1979).
[13] D. J. Tannor and E. J. Heller, J. Chem. Phys. **77**, 202 (1982).
[14] T. Petrenko and F. Neese, J. Chem. Phys. **137**, 234107 (2012).
[15] D. W. Silverstein and L. Jensen, J. Chem. Phys. **136**, 064111 (2012).
[16] H. Ma, J. Liu, and W. Liang, J. Chem. Theory Comput. **8**, 4474 (2012).
[17] A. Baiardi, J. Bloino, and V. Barone, J. Chem. Phys. **141**, 114108 (2014).
[18] J. Mattiat and S. Luber, J. Chem. Phys. **149**, 174108 (2018).
[19] F. J. A. Ferrer, V. Barone, C. Cappelli, and F. Santoro, J. Chem. Theory Comput. **9**, 3597 (2013).
[20] F. Egidi, J. Bloino, C. Cappelli, and V. Barone, J. Chem. Theory Comput. **10**, 346 (2014).
[21] P. Yang, D. Qi, G. You, W. Shen, M. Li, and R. He, J. Chem. Phys. **141**, 124304 (2014).
[22] W. Liang, H. Ma, H. Zang, and C. Ye, Int. J. Quantum Chem. **115**, 550 (2015).
[23] M. Walter and M. Moseler, J. Chem. Theory Comput. **16**, 576 (2020).
[24] J. Guthmuller, J. Chem. Phys. **148**, 124107 (2018).
[25] F. Santoro, A. Lami, R. Improta, J. Bloino, and V. Barone, J. Chem. Phys. **128**, 224311 (2008).
[26] P. M. Johnson, H. Xu, and T. J. Sears, J. Chem. Phys. **125**, 164330 (2006).
[27] D. L. Tonks and J. B. Page, Chem. Phys. Lett. **66**, 449 (1979).
[28] M. J. Frisch, G. W. Trucks, H. B. Schlegel, G. E. Scuseria, M. A. Robb, J. R. Cheeseman, G. Scalmani, V. Barone, G. A. Petersson, H. Nakatsuji, X. Li, M. Caricato, A. V. Marenich, J. Bloino, B. G. Janesko, R. Gomperts, B. Mennucci, H. P. Hratchian, J. V. Ortiz, A. F. Izmaylov, J. L. Sonnenberg, D. Williams-Young, F. Ding, F. Lipparini, F. Egidi, J. Goings, B. Peng, A. Petrone, T. Henderson, D. Ranasinghe, V. G. Zakrzewski, J. Gao, N. Rega, G. Zheng, W. Liang, M. Hada, M. Ehara, K. Toyota, R. Fukuda, J. Hasegawa, M. Ishida, T. Nakajima, Y. Honda, O. Kitao, H. Nakai, T. Vreven, K. Throssell, J. J. A. Montgomery, J. E. Peralta, F. Ogliaro, M. J. Bearpark, J. J. Heyd, E. N. Brothers, K. N. Kudin, V. N. Staroverov, T. A. Keith, R. Kobayashi, J. Normand, K. Raghavachari, A. P. Rendell, J. C. Burant, S. S. Iyengar, J. Tomasi, M. Cossi, J. M. Millam, M. Klene, C. Adamo, R. Cammi, J. W. Ochterski, R. L. Martin, K. Morokuma, O. Farkas, J. B. Foresman, and D. J. Fox, Gaussian 16, Revision C.01, Gaussian, Inc., Wallingford, CT, 2019.
[29] P. T. Ruhoff, Chem. Phys. **186**, 355 (1994).
[30] D. L. Phillips, M. Z. Zgierski, and A. B. Myers, J. Phys. Chem. **97**, 1800 (1993).
[31] R. J. Hemley, J. I. Dawson, and V. Vaida, J. Chem. Phys. **78**, 2915 (1983).
[32] R. McDiarmid and A.-H. Sheybani, J. Chem. Phys. **89**, 1255 (1988).
[33] R. R. Chadwick, M. Z. Zgierski, and B. S. Hudson, J. Chem. Phys. **95**, 7204 (1991).
[34] C.-P. Hsu, S. Hirata, and M. Head-Gordon, J. Phys. Chem. A **105**, 451 (2001).
[35] R. P. Krawczyk, K. Malsch, G. Hohlneicher, R. C. Gillen, and W. Domcke, Chem. Phys. Lett. **320**, 535 (2000).
[36] A. Komainda, B. Ostojić, and H. Köppel, J. Phys. Chem. A **117**, 8782 (2013).
[37] A. Komainda, D. Lefrancois, A. Dreuw, and H. Köppel, Chem. Phys. **482**, 27 (2017).
[38] A. E. Boguslavskiy, O. Schalk, N. Gador, W. J. Glover, T. Mori, T. Schultz, M. S. Schuurman, T. J. Martínez, and A. Stolow, J. Chem. Phys. **148**, 164302 (2018).
[39] W. J. Glover, T. Mori, M. S. Schuurman, A. E. Boguslavskiy, O. Schalk, A. Stolow, and T. J. Martínez, J. Chem. Phys. **148**, 164303 (2018).
[40] R. McDiarmid, J. Chem. Phys. **64**, 514 (1976).